Environ Monit Assess (2023) 195:1081
https://doi.org/10.1007/s10661-023-11697-6

RESEARCH

An integrative data-driven approach for monitoring corn biomass under irrigation water and nitrogen levels based on UAV-based imagery

Farid Feizolahpour · Sina Besharat · Bakhtiar Feizizadeh · Vahid Rezaverdinejad · Behzad Hessari

Received: 2 September 2022 / Accepted: 8 August 2023

Abstract Unmanned aerial vehicle (UAV)-based remote sensing has been widely considered recently in field scale crop yield estimation. In this research, the capability of 13 spectral indices in the form of 5 groups was studied under different irrigation water and N fertilizer managements in terms of corn biomass monitoring and estimation. Farm experiments were conducted at Urmia University, Iran. The research was done using a randomized complete block design at three levels of 60, 80, and 100% of irrigation water and nitrogen requirements during four replications. The aerial imagery operations were performed using a fixed-wing UAV equipped with a Sequoia sensor during three plant growth stages including stem elongation, flowering, and silking. The effect of different irrigation water and nitrogen levels on vegetation indices and crop biomass was examined using variance decomposition analysis. Then, the correlation of the vegetation indices with corn biomass was evaluated by fitting linear regression models. Based on the obtained results, the indices based on near infrared (NIR) and red-edge spectral bands showed a better performance. Thus, the MERIS terrestrial chlorophyll index (MTCI) indicated the highest accuracy at estimating corn biomass during the growing season with the R^2 and RMSE values of 0.92 and 8.27 ton/ha, respectively. Finally, some Bayesian model averaging (BMA) models were proposed to estimate corn biomass based on the selected indices and different spectral bands. Results of the BMA models revealed that the accuracy of biomass estimation models could be improved using the capabilities and advantages of different vegetation indices.

Keywords Bayesian model averaging · Biomass · Corn · Remote sensing · Unmanned aerial vehicle · Vegetation index

F. Feizolahpour · S. Besharat (✉) · V. Rezaverdinejad · B. Hessari
Department of Water Engineering, Faculty of Agriculture, Urmia University, Urmia, Iran
e-mail: s.besharat@urmia.ac.ir

F. Feizolahpour
e-mail: farid.feizolahpour@gmail.com

V. Rezaverdinejad
e-mail: v.verdinejad@urmia.ac.ir

B. Hessari
e-mail: b.hessari@urmia.ac.ir

S. Besharat
Water Engineering Department of Urmia Lake Research Institute, Urmia, Iran

B. Feizizadeh
Faculty of Planning and Environmental Sciences, Department of Remote Sensing and Geographical Information System (GIS), University of Tabriz, Tabriz, Iran
e-mail: Feizizadeh@tabrizu.ac.ir

B. Hessari
Environment Department of Urmia Lake Research Institute, Urmia, Iran

Published online: 24 August 2023

Introduction

The rapid growth of the global population and limitations in soil and water resources have highlighted the importance of precision agriculture and water productivity. Accurate prediction of vegetation biomass and yield ahead of harvesting enables planners to improve national food policies and apply a more appropriate management (Noureldin et al., 2013). One of the typical methods for determining the plant yield is using destructive measurement methods, which are time consuming, costly, and challenging due to farm sampling (Afshar et al., 2021a, b). On the other hand, the availability and capability of aerial and satellite datasets have turned remote sensing into a big data technology with enormous applications in agricultural sciences and specially crop yield monitoring (Feizizadeh et al., 2021; Xu et al., 2021). In this regard, many desirable results have been achieved in monitoring vegetation conditions and crop biomass estimation by using spectral vegetation indices (Afshar et al., 2021a, b; Carneiro et al., 2019; Chen et al., 2019; Zhou et al., 2017).

In recent years, many studies have been done on monitoring crop performance and conditions using satellite images. In one research, Wang et al. (2010) suggested models for predicting rice yield at the plant potting phase using spectral vegetation ratios such as NIR/red and NIR/green. These models showed acceptable results in estimating rice yield on a large scale by using satellite images. Baio et al. (2018) also reported a positive linear relationship between the normalized difference vegetation index (NDVI) and cotton yield. Further, in other studies carried out by Becker-Reshef et al. (2010), Mkhabela et al. (2011), Bolton and Friedl (2013), and Huang et al. (2013), different crop yield regression models have been developed based on NDVI. Zhou et al. (2020) also presented an approach based on spatiotemporal data fusion by fusing Sentinel-2 and Sentinel-3 data to reconstruct field-scale leaf area index (LAI) imagery over the growth period of winter wheat. Further, Tian et al. (2020) have reported that continuous measurement of LAI is very crucial for winter wheat yield estimation. Zhao et al. (2020) also reported that on farm scale, a prediction model based on NDVI, soil-adjusted vegetation index (OSAVI), and enhanced vegetation index (EVI) vegetation indices resulting from Sentinel-2 had a better performance in comparison to the prediction of wheat yield using one or multiple vegetation indices. Similarly, other studies have been performed using other spectral indices such as the normalized difference water index (NDWI) (Bolton & Friedl, 2013), EVI (Duncan et al., 2015), the modified chlorophyll absorption ratio index (MCAR), and the transformed chlorophyll absorption ratio index (TCARI) (Sharifi, 2020). Nonetheless, it should be noted that in each experimental approach, using equations in new locations or at other times can be challenging (Lobell, 2013).

As mentioned before, utilizing satellite images has led to acceptable accuracy and performance in estimating the plant yield at a large scale. Nevertheless, in most regions, problems such as small farm size, improper topography, bad climate during the growing season, huge costs, and limitations in accessing data have impeded the application of satellite remote sensing (Zhang & Kovacs, 2012; Zhou et al., 2017). Capabilities of the unmanned aerial system (UAS) in terms of spatial-time resolution, low cost, ease of use, and application of different sensors have developed this system for improving precision farming (Zhang & Kovacs, 2012). Meanwhile, several research studies have been conducted using UAVs to monitor vegetation conditions, diagnose diseases, examine vegetation stresses, and do phenotyping (Córcoles et al., 2013; Fullana-Pericàs et al., 2022; Ihuoma & Madramootoo, 2017; Verger et al., 2014; Zhao et al., 2018; Zhou et al., 2021).

In addition, there are several studies in the field of crop yield estimation using UAV aerial images based on different vegetation indicators. Teoh et al. (2016) and Maresma et al. (2020) have reported that NDVI derived from UAV aerial images is highly correlated with crop yield. Zhou et al. (2017) used UAV spectral images during several stages of plant growth and concluded that indices highly correlated with LAI have a better performance in crop yield estimating. Carneiro et al. (2019) studied three vegetation indices such as NDVI, the normalized difference red-edge index (NDRE), and the infrared percentage vegetation index (IRVI) to evaluate the spatial-time changes of soy plants. According to the findings, the best time for obtaining data was 45 and 60 days after plantation, and NDRE showed a better performance than other indices. Yeom et al. (2019) also used 13 different vegetation indices derived from UAV data to analyze the effect of tillage on plant health and vegetation

index performance. NIR-based indices indicated a better performance than RGB-based ones, and the modified soil adjusted vegetation index (MSAVI) had the best performance. In addition, one research conducted based on different field managements comprising six various treatments of nitrogen, potassium, and combined fertilizers showed that potato yield could be estimated using four vegetation indices with a correlation coefficient of 0.63 for the image data set of 90 days after planting (Li et al., 2020). Furthermore, Duan et al. (2021) concluded that multi-temporal vegetation index (VI) grain yield estimation models could be more accurate than single-stage Vls in estimating different rice cultivars. On the other hand, some studies have been conducted to predict crop yield using plant height. In this regard, crop surface models (CSMs) have been developed to estimate plant height using digital images (Bendig et al., 2015; Geipel et al., 2014). Nevertheless, it has been observed that height-yield relationships change significantly under different variants and during various growing stages (Zhou et al., 2017).

A review and evaluation of research history indicate that numerous studies conducted using vegetation indices derived from different data acquisition equipment (LiDAR, RGB, multispectral and hyperspectral sensors) and various data analysis methods such as regression techniques, ANN, SVR, and RFR. Despite rapid developments in remote sensing and accessibility of UAV images, difficulties have remained and there is no global method to apply for all crops in all cases. Although multi-sensor data fusion improves the accuracy of crop monitoring, it makes the process of data collection more complex and difficult, which can lead to reducing the speed of monitoring. Also, although advanced analysis methods improve evaluation accuracy, they require a long training time and will have poor performance in small sample sizes and lack of samples. On the other hand, different farming management and different crops, even the same crops in different environments, have different characteristics and can be effective on crop reflectance and spectral indices. These differences require us to carefully distinguish the features of crops, use appropriate sensors to collect features, and test multiple indices to determine the best biomass indices. We hypothesize that different VIs developed from aerial imagery collected using UAV would have a significant and specific relationship with corn biomass and the accuracy of biomass estimation can be improved by Bayesian averaging of VIs during crop growth stages. Therefore, the main objectives of this research were to (i) analyze the effect of different irrigation and nitrogen levels on biomass and UAV spectral indices, (ii) examine the efficiency of the most widely used spectral indices during different plant growth stages, and (iii) improve the accuracy of biomass estimation models by using the BMA combined approach.

Materials and methods

Research area and experimental treatments

In this research, farm experiments were performed in part of the research field of Urmia University, West Azerbaijan, Iran, with an area of 4800 square meters, coordinates 37°39′18.85″ N, 44°58′20.39″ E (UTM 497,559.37 m E, 4,167,564.23 m N, zone: 38 S), and the elevation of 1370 m, during the 2017–2018 growing season. The farm had a uniform topography with a mild slope of 0.1 m/m and a deep groundwater level (Fig. 1). The average annual rainfall in Urmia was 308 mm, and the minimum and maximum long-term temperatures were 5.3 and 18.1 °C, respectively, with a semi-arid climate. To determine the farm soil's physical and chemical properties, samples were extracted from different soil depths before plantation and tested in the laboratory. Some physical and chemical properties of the farm soil are listed in Table 1.

Farm experiments were carried out based on a randomized block factorial design with nine treatments in four replications. The first factor included three levels of irrigation (I1 = 100%, I2 = 80%, and I3 = 60% of crop water requirement); the second one involved three levels of nitrogen application (N1 = 100%, N2 = 80%, and N3 = 60% of N fertilizer requirement). Thus, T1 to T9 treatments defined as T1: I1N1, T2: I1N2, T3: I1N3, T4: I2N1, T5: I2N2, T6: I2N3, T7: I3N1, T8: I3N2, and T9: I3N3. According to the soil composition test and the fertilization recommendation, the amount of the consumed urea fertilizer was determined to be 250 kg/ha; other treatments were specified as a percentage of this amount. The details of the treatments and also the workflow of the research are shown in Fig. 2.

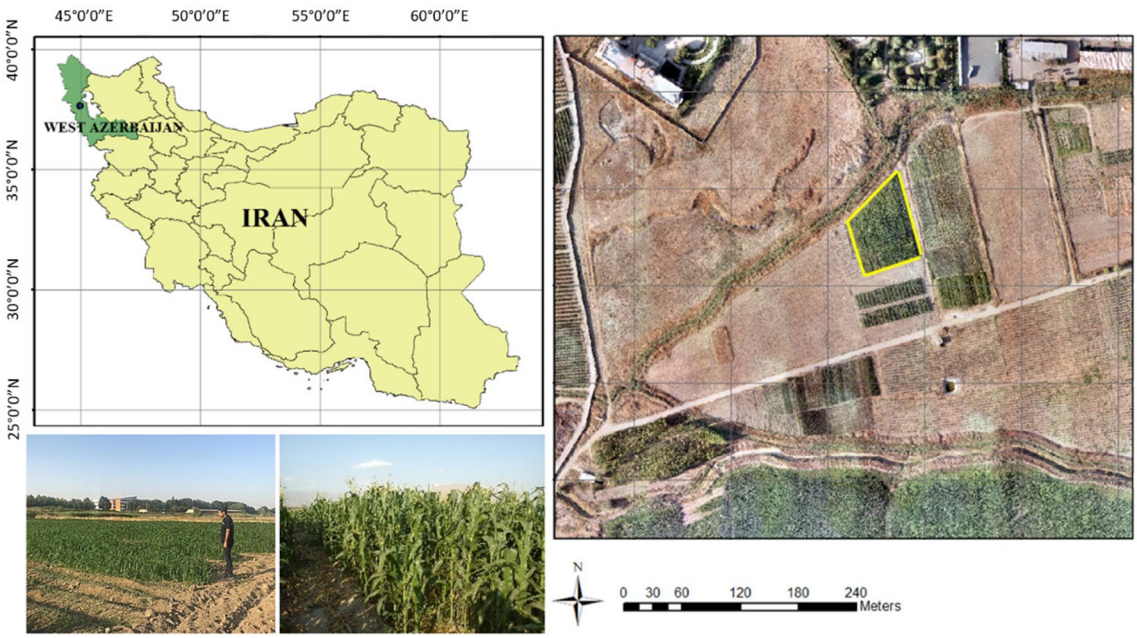

Fig. 1 Location of the research area

In order to estimate the evapotranspiration of the reference crop, the Penman-Monteith equation based on the FAO-56 method was used. Based on this, the corn irrigation requirement was estimated to be equal to 610 mm/season for the 100% water requirement treatment (I1); the amount of the required irrigation water for other treatments was determined based on this value. Irrigation operation was then performed using a T-tape drip irrigation system.

Each experimental plot included six planting rows with a width of 50 cm and a length of 15 m. The distances between the plots were considered to be between 1.5 and 2 m to overcome the effect of the humidity of different irrigation levels. Double-cross maxima 580 hybrid cultivars were used to plant corn with 25-cm distances in rows (Fig. 3).

Data collection

In this research, an eBee+ fixed-wing UAV equipped with a Sequoia multispectral sensor having four spectral bands of green, red, infrared, and red-edge was used (Fig. 3). All flight parameters, including ran strips, imaging stations, flight height, longitudinal and latitudinal overlap in images, ground sampling distance (GSD) dimensions of the image, flight time, and flight distance, were determined using the emotion3D software. Thus, GSD dimensions of the images, flight height, and longitudinal and latitudinal overlap between images were considered to be 10 cm, 110 m, and 80 and 70%, respectively.

Table 1 Test result of physical and chemical properties of soil

Soil depth (cm)	Soil texture	Total N (%)	Organic carbon (%)	Potassium (ppm)	Phosphorous (ppm)	Salinity (dS/m)	pH (-)	Field capacity (cm^3/cm^3)	Permanent wilting point (cm^3/cm^3)
0–30	Silty clay	0.11	1.28	485	11.2	0.65	8.2	0.383	0.208
30–60	Clay	0.05	0.60	379	5.2	0.45	8.2	0.415	0.223

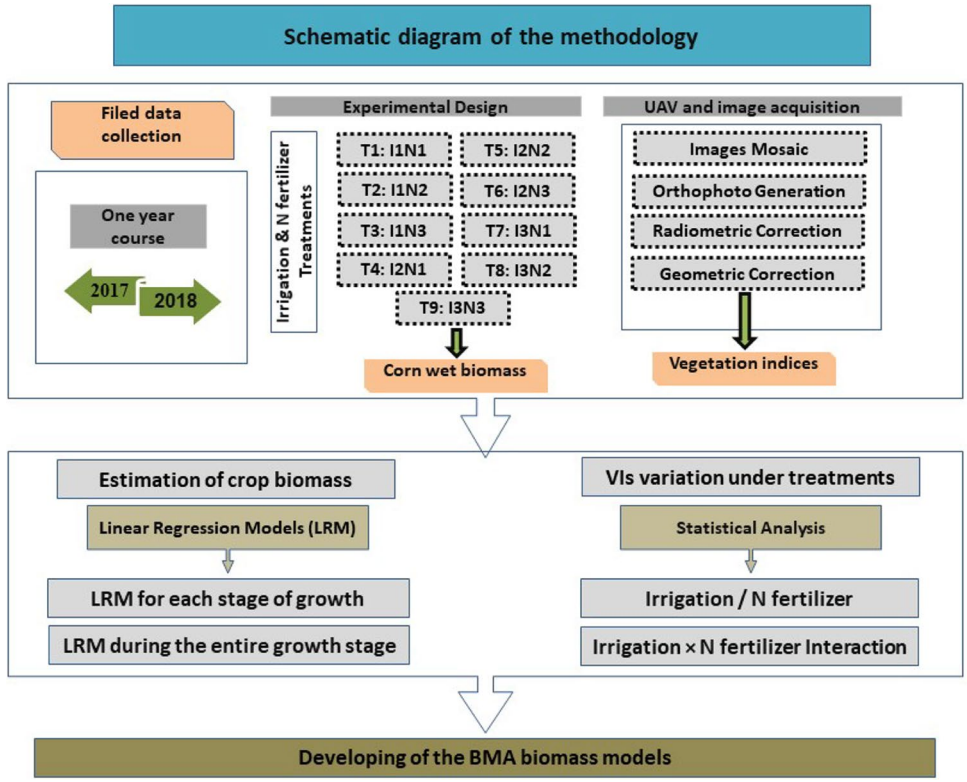

Fig. 2 Work flow of the methodology used in this research

Vegetation indices

In this section, the obtained images were pre-processed in terms of geometric correction and mosaicking of the image using the Pix4Dmapper software to extract the vegetation indices. Pix4D-Mapper software is UAS photography geometric correction and mosaic technology based on feature

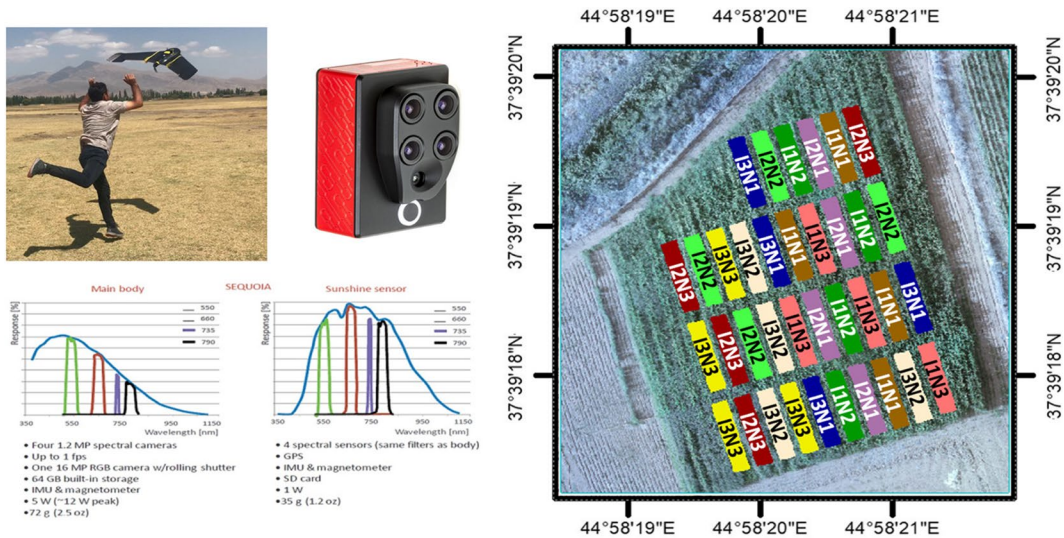

Fig. 3 Flight operation and experimental treatments

matching and structure from motion (SfM) photogrammetry technology (Turner et al., 2012). Initially, images were processed in a model space to create three-dimensional point clouds. The point cloud was then used to generate the digital terrain model (DTM) required for image correction. Subsequent geographic reference images linked together to form the mosaic of the study area. Finally, after performing the required preprocessing, 13 vegetation indices were estimated in the form of 5 groups based on the relations presented in Table 2.

Crop harvesting and statistical analysis of the data

At the end of the growing season, crop samples were obtained from four rows of middle plantations and the weight of the biomass was calculated as the fresh weight of the plant. Also, the spectral samples of the treatments were extracted from UAV images simultaneously with crop samplings during three plant growth stages including stem elongation (F1), flowering (F2), and silking (F3). Finally, to determine the effectiveness of the treatments, the

Table 2 The utilized vegetation indices for monitoring vegetation condition

Ref.	Equation	Bands	Group	Index
Tucker (1979)	$(green - red)/(green + red)$	Green, red	1	GRVI (green red vegetation index)
Bendig et al. (2015)	$(green^2 - red^2)/(green^2 + red^2)$			MGRVI (modified green red vegetation index)
Gitelson et al. (2003)	$(nir - green)/green$	Green, NIR	2	GCI (green chlorophyll index)
Gitelson et al. (2003)	$(nir - green)/(nir + green)$			GNDVI (green normalized difference vegetation)
Rouse et al. (1974)	$(nir - red)/(nir + red)$	Red, NIR	3	NDVI (normalized difference vegetation)
Huete (1988)	$1.5 \times (nir - red)/(nir + red + 0.5)$			SAVI (soil adjusted vegetation index)
Qi et al. (1994)	$0.5 \times (2nir + 1 - \sqrt{(2nir + 1)^2 - 8(nir - red)})$			MSAVI (modified soil adjusted vegetation index)
Peñuelas et al. (1994)	$1.16 \times (nir - red)/(nir + red + 0.16)$			OSAVI (optimized soil adjusted vegetation index)
Gitelson et al. (2003)	$(0.2 \times nir - red)/(0.2 \times nir + red)$			WDRVI (wide dynamic range vegetation index)
Jiang et al. (2008)	$2.5 \times (nir - red)/(1 + nir + 2.4 \times red)$			EVI2 (enhanced vegetation index 2)
Gitelson and Merzlyak (1994)	$(nir - rededge)/(nir + rededge)$	NIR, red edge	4	NDRE (normalized difference red-edge index)
Gitelson et al. (2003)	$(nir/rededge) - 1$			RECI (red-edge chlorophyll index)
Dash and Curran (2004)	$(nir - rededge)/(rededge - red)$	Red, red edge, NIR	5	MTCI MERIS terrestrial chlorophyll index

variance decomposition technique (ANOVA) was used by applying the SPSS statistical software; also, the treatment means were compared using Duncan's multiple range test.

Model development

Development of linear regression models

In addition to examining the effect of irrigation water and nitrogen levels on VIs, the capability of these indices in estimating crop biomass was investigated as well. In this regard, simple linear regression models between spectral indices and vegetation biomass were developed as independent and dependent variables, respectively. The first approach in regression equations' fitting was to estimate plant biomass during different growing season stages and compare the indices during the growth season. Therefore, linear regression relationships were proposed individually for the first, second, and third stages of the aerial survey. On the other hand, the second approach was developing regression models for the entire growing season, considering that the planting date of plants might be different in a vast area.

Development of the combined model using the BMA method

In crop biomass modeling by using various indices, uncertainty in the input data may cause multiple outcomes and bring uncertainty in the final results. In most cases, it is attempted to choose one of the models using statistical methods and simulate data by these models, which can cause an error due to the possibility of other scenarios. Hence, considering the models' outcomes and possible scenarios in simulation can increase the accuracy and raise the reliability of the model's predictions. One of the most common methods used for combining model results is the Bayesian model averaging (BMA) method, which was carried out in R (version 3.5.1). In this method, it is assumed that all models are beneficial and can be used in simulation; however, the degree of certainty is different, such that it can be defined by attributing weight to each. The weight of each simulation and the variance of their distribution function are determined using the posterior probability distribution function of each. Then, by using the defined weights, one of the simulation models is selected and a random number is chosen using their distribution function. The weight of each simulation depends on its correlation with the observation data, as measured by the posterior probability of each model. If we assume that f1, f2, …, and fk are simulation models (simulated scenarios) and their distribution function is gk(y|fk), then the BMA predictor model is defined as shown below (Hoeting et al., 1999; Raftery et al., 2005):

$$P(y|f_1,...,f_k) = \sum_{k=1}^{k} w_k g_k(y|f_k) \quad (1)$$

where w_k is the possibility of choosing simulation k as the best simulation, which is determined based on the performance of the simulation k. These values have probabilistic characteristics in such a way that each is non-negative and the sum of all of them is equal to one ($\sum_{k=1}^{k} w_k = 1$).

Assessment criteria of the models' performance

In this research, to evaluate the obtained results, two common statistical indices, including root mean square error (RMSE) and coefficient of determination (R^2), were used:

(Willmott & Matsuura, 2005)

$$RMSE = \sqrt{\sum_{k=1}^{N} \frac{(X_k - Y_k)^2}{N}} \quad (2)$$

(Zou et al., 2003)

$$R^2 = \left[\frac{\sum_{k=1}^{N} (X_k - \overline{X})(Y_k - \overline{Y})}{\sum_{k=1}^{n} (X_k - \overline{X})^2 \sum_{k=1}^{N} (Y - \overline{Y})^2} \right]^Z \quad (3)$$

where N is the sum of data, X is the calculated output, Y is the measured output, and $\overline{X}$ and $\overline{Y}$ are the average values.

Results

Variations of VIs under various experimental treatments

Figure 4 represents the results of the 13 spectral indices obtained during three aerial surveys, along with the reflectance changes of the related bands for each index. As can be seen, changes in the indices during the growing season were not similar. Indices of groups 1 and 2 and some of group 3, such as NDVI,

OSAVI, and WDRVI, showed a different behavior, as compared to other indices. These values were higher during the start of the season and did not change in the second stage in comparison to the end of the season. Also, the evaluation of VIs during different treatments showed that the effect of different irrigation water and N fertilizer levels on VIs was different. For example, the obtained values of GRVI and MGRVI for the T1 treatment with 100% of irrigation water and the N fertilizer requirement were not the highest during the second and third flights in contrast to other indices; also, they were lower than other treatments. Nonetheless, values of green, red, red-edge, and NIR spectral bands showed a similar behavior; their values were more in the second flight than in the first one; also, they were higher in the third flight rather than the second one, which was in accordance with the plant growth.

Based on Fig. 4, the indices of group 1 decreased during the growing season; the highest values of

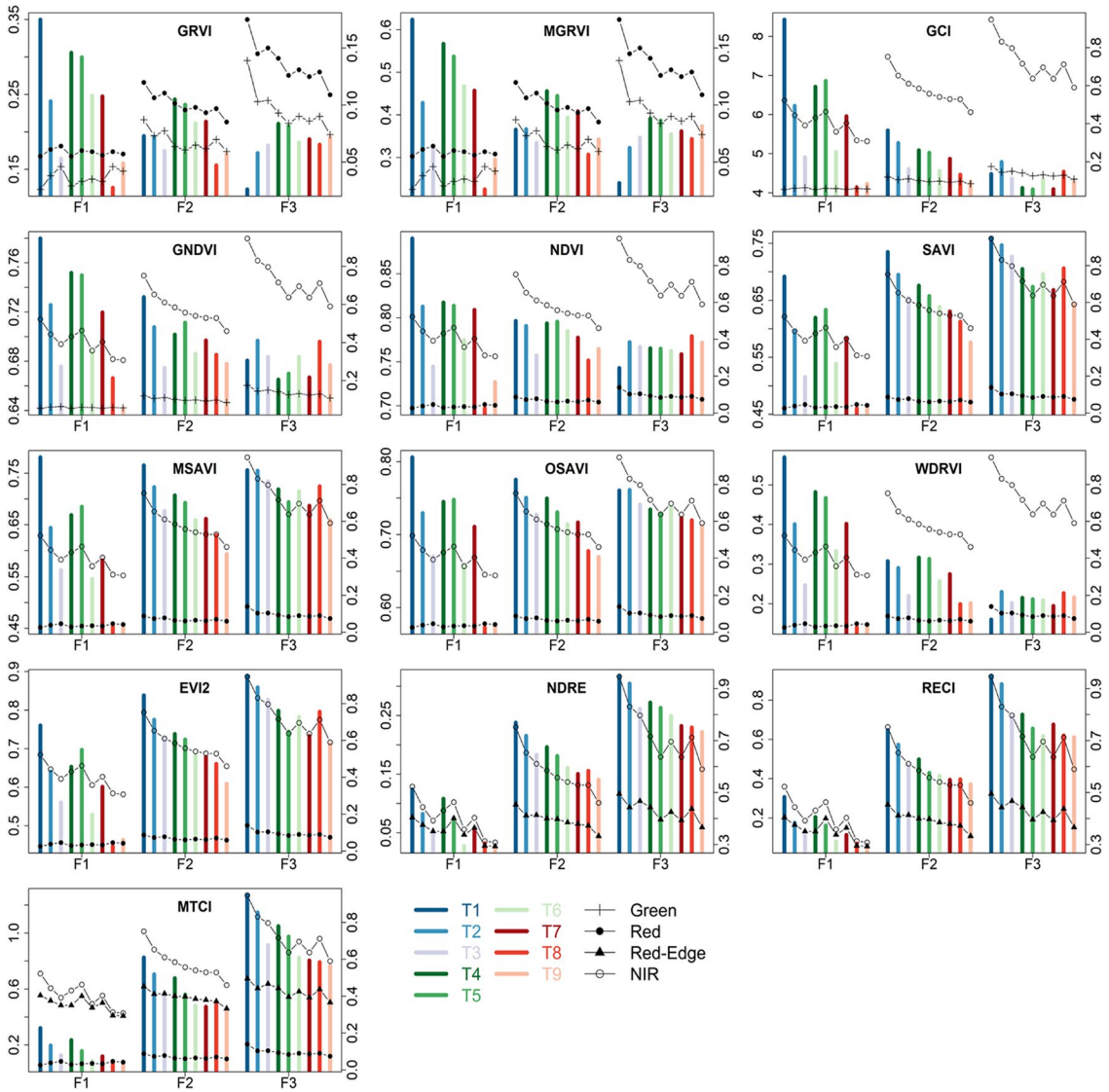

Fig. 4 Vegetation indices and spectral bands under different treatments during the growing season (F1, flight1; F2, flight2; and F3, flight3 during first, second, and third stages of measurements)

GRVI and MGRVI were in the first flight at the beginning of the growing season. Meanwhile, despite plant growth and an increase in the green and red bands during the second and third flights, the values of the indices obtained from these bands had a decreasing trend. Similarly, the indices of group 2 also had the highest values at the beginning of the growing season; in the following stages of plant growth, their values decreased in most treatments despite the increase of the green and NIR spectral bands. Among the indices of group 3, NDVI, WDRVI, and OSAVI showed a behavior different from that of SAVI, MSAVI, and EVI2. These differences were due to mathematical relationships and different coefficients considered for red and NIR bands. Most indices of group 3 had high values at the beginning of the growing season, not showing a significant change during the second and third flights; they were saturated at the end of the growing season. Unlike other indices, during the third flight, WDRVI exhibited a large decline, as compared to the second and first flights; in contrast, EVI2 was increased during the second and third flights, as compared to the previous stage.

Examination of the indices in groups 4 and 5 showed that NDRE, RECI, and MTCI increased with increasing the red, red-edge, and NIR bands during the growing season; however, they did not reach a saturation state in the third stage. One of the most important reasons for this issue is using the red-edge spectral band, which is highly sensitive to leaf chlorophyll, increasing with plant growth.

Statistical analysis of the effect of irrigation water and nitrogen application levels on corn biomass and VIs

Based on the variance decomposition results, the effects of irrigation water and N fertilizer levels and the interaction of irrigation water × N fertilizer on corn biomass were significant during three flights ($p < 0.01$). However, the effect of irrigation and N fertilizer levels on VIs was different; the obtained results, thus, indicated the importance of the utilized spectral bands.

In addition, the results of comparing the means of irrigation water and N fertilizer levels are presented in Table 3. As can be seen, the biomass of corn decreased significantly with the reduction of irrigation and N fertilizer levels during all three stages; the highest value was obtained at a level of 100% of irrigation water and N fertilizer requirement. Based on the results of stage 3, the average crop biomasses for I1, I2, and I3 treatments were 84.809, 80.488, and 67.667 ton/ha, respectively; meanwhile, these values for N1, N2, and N3 treatments were 89.074, 75.361, and 68.529 ton/ha, respectively.

However, examining the effect of different irrigation water and N fertilizer levels on some VIs showed a different result. Unlike corn biomass, GRVI had the highest values at I2 treatments with 80% of irrigation water requirement during the second and third stages; the highest MGRVI values were achieved at I2 treatments during all measurement stages. On the other side, these indices were decreased in accordance with a decline in the consumed N fertilizer during the first and second measurement stages; it was only in the third stage that N2 and N3 treatments with 80 and 60% of the N fertilizer requirement showed a larger value, as compared to N1 treatments, with 100% of the N fertilizer requirement. In the same way, the maximum values of GCI and GNDVI indices were obtained at I1 and N1 treatments; it was only in N2 treatments that a larger value was observed, as compared to other levels. Furthermore, as shown in Fig. 4, the values of the indices of groups 1 and 2 decreased over time despite plant growth. Meanwhile, the values of the third and second measurement stages were obtained to be less than those of the first stage. Therefore, using the green and red bands could not correctly depict the level of plant growth and biomass of corn by irrigation water and N fertilizer levels during the growing season.

As can be seen in Table 3, among indices of group 3, NDVI and WDRVI showed a weaker performance than other ones. Throughout all measurement stages, NDVI did not show a significant difference between I1 and I2 treatments with 100 and 80% of irrigation water requirement levels; at the third measurement stage, the value of this index for N3 and N2 treatments was higher than that in N1 treatments. On the contrary, EVI2 and MSAVI showed a better performance than other indices; in most cases, they could show a significant difference between irrigation and N fertilizer levels.

Examination of the values of groups 4 and 5 indices showed that these indices had significant variations in regard to the changes in irrigation water and N fertilizer application levels; in all measurement stages, they achieved the maximum values in I1 and

Table 3 Mean values of corn biomass and VI response to irrigation water and N fertilizer levels

Irrigation water levels															
Biomass	**MTCI**	**RECI**	**NDRE**	**EVI2**	**WDRVI**	**OSAVI**	**MSAVI**	**SAVI**	**NDVI**	**GNDVI**	**GCI**	**MGRVI**	**GRVI**	**Level**	
10.941a	0.214a	0.205a	0.087a	0.654a	0.406a	0.735a	0.663a	0.601a	0.816a	0.727a	6.518a	0.458a	0.284a	100	Flight1
10.241b	0.159b	0.148b	0.07b	0.626b	0.427b	0.717b	0.633b	0.597a	0.802a	0.729a	6.203b	0.523b	0.252b	80	
9.558c	0.083c	0.079c	0.038c	0.504c	0.228c	0.619c	0.496c	0.502b	0.744b	0.676b	4.774c	0.326c	0.177c	60	
40.428a	0.701a	0.563a	0.212a	0.779a	0.272b	0.75a	0.722a	0.694a	0.781a	0.704a	5.157a	0.355b	0.187b	100	Flight2
38.862b	0.573b	0.447b	0.179b	0.714b	0.295a	0.731b	0.686b	0.657b	0.791a	0.699ab	4.886b	0.431a	0.230a	80	
30.240c	0.469c	0.387c	0.149c	0.649c	0.225c	0.687c	0.628c	0.606c	0.764b	0.686b	4.534c	0.352b	0.179c	60	
84.809a	1.110a	0.838a	0.294a	0.857a	0.197b	0.754a	0.748a	0.744a	0.761a	0.687a	4.541a	0.303c	0.158c	100	Flight3
80.488b	0.948b	0.665b	0.261b	0.775b	0.212a	0.733b	0.709b	0.691b	0.764a	0.672b	4.181c	0.377a	0.201a	80	
67.667c	0.787c	0.635c	0.228c	0.747c	0.211a	0.717c	0.69c	0.672c	0.769a	0.679b	4.303b	0.359b	0.188b	60	
N fertilizer levels															
10.662a	0.224a	0.208a	0.096a	0.671a	0.484a	0.754a	0.677a	0.631a	0.838a	0.750a	7.032a	0.549a	0.301a	100	Flight1
10.276b	0.142b	0.135b	0.063b	0.595b	0.336b	0.683b	0.594b	0.564b	0.774b	0.714b	5.74b	0.397b	0.222b	80	
9.802c	0.089c	0.089c	0.037c	0.517c	0.242c	0.634c	0.52c	0.505c	0.749c	0.668c	4.723c	0.361c	0.19c	60	
42.299a	0.658a	0.513a	0.195a	0.751a	0.299a	0.747a	0.711a	0.680a	0.789a	0.710a	5.181a	0.409a	0.217a	100	Flight2
37.084b	0.585b	0.466b	0.184b	0.719b	0.267b	0.719b	0.682b	0.655b	0.779ab	0.701a	4.918b	0.372b	0.195b	80	
29.931c	0.501c	0.418c	0.161c	0.672c	0.226c	0.703c	0.643c	0.623c	0.769b	0.679b	4.478c	0.357c	0.185c	60	
89.074a	1.041a	0.774a	0.274a	0.806a	0.190c	0.736a	0.720a	0.710a	0.755b	0.671b	4.229c	0.331b	0.175b	100	Flight3
75.361b	0.971b	0.718b	0.265b	0.799a	0.223a	0.735a	0.724a	0.708a	0.772a	0.687a	4.469a	0.351a	0.187a	80	
68.529c	0.834c	0.647c	0.244c	0.773b	0.209b	0.729a	0.702b	0.688b	0.767a	0.681a	4.326b	0.358a	0.186a	60	

N1 treatments with 100% of irrigation water and N fertilizer requirement. Also, their values were significantly more in 80 rather than 60% of irrigation water requirement treatments. Further, while indices of the first, second, and third groups at the end of the growing season did not show a significant change between levels 80–100 and 60–80% of the N fertilizer requirement, NDRE, RECI, and MTCI resulted in a significant difference between all levels of irrigation water and N fertilizer, thus leading to better results. This was due to using the red-edge band in these indices, which was sensitive to plant chlorophyll, creating significant differences when using different N fertilizer levels. Other similar studies have shown that NDRE could have a better performance than NDVI in identifying the inhomogeneities of olive vegetation (Jorge et al., 2019).

For a more detailed examination, the results of comparing the means analysis for corn biomass and the five best indices of each group are represented individually for each treatment in Fig. 5. A research of the results related to corn biomass indicated that the T1 treatment with 100% of irrigation water and N fertilizer requirement had the highest biomass during the entire plant growing season; its values for the first to third measurements were, respectively, 11.462, 45.980 and 96.263 ton/ha. Additionally, in the last measurement stage, it was observed that after T1, the highest crop biomass was equal to 92.008 and 81.515 ton/ha for T4 and T2 treatments, respectively; T9 had the lowest crop biomass when using 60% of irrigation water and N fertilizer requirement. Based on the results of the research done by Lisar et al. (2012) and Viero et al. (2017), water stress intensifies the chlorophyll stresses in plant leaves since nutrition transportation in a plant is done via water; also, a reduction in plant water content increases nitrogen losses due to volatilization.

Also, it was observed that during the first and second measurement stages, GCI of the T1 treatment was significantly higher than that in other treatments; however, in the third stage, T2 had the highest value of this index. Thus, the maximum values of GCI in the first, second, and third measurement stages were 8.428, 5.594, and 4.786, respectively. Hence, this index had an acceptable performance during the plant's primary growing stages; however, it should be noted that its value decreased along with the crop growth; therefore, it should not be used in researching two regions with different plantation times. Similarly, GRVI had an acceptable performance during the primary stage, appropriately showing the vegetation state according to biomass and crop growing conditions. However, during the second and third measurement stages, T4 and T5 had the largest amount of GRVI; even in the third stage, the value of this index in T9 was significantly higher than that in T1 and T2, thus signifying the low accuracy of this index at the end of the growing season.

Investigation of EVI2, RECI, and MTCI changes showed that the behavior of these indices was similar; contrary to GCI and MGRVI, their values increased as the plant grew during the growing season. In all measurement stages, the maximum value of these indices occurred in T1; in most cases, they directly changed following the variation in the crop biomass. For example, as can be seen in the color image of MTCI (Fig. 5), in the third flight, similar to the crop biomass behavior, the highest values of this index resulted in the treatments T1, T2, and T3, which were 1.269, 1.049, and 1.147, respectively; meanwhile, the lowest values were observed in T8 and T9, with the values of 0.620 and 0.611, respectively. In some cases, this did not occur; changes in indices were not in accordance with those in the biomass level. For instance, EVI2 of T8 in the third measurement stage was more than its value on T5, T6, and T7. Meanwhile, the amount of biomass in T8 was less than that in the mentioned treatments.

Estimation of crop biomass using vegetation indices

The relationships between corn biomass and 13 spectral indices during three growing stages and the entire growing season were analyzed (Fig. 6). Based on the obtained results in the first stage, indices of groups 4 and 5 showed a better performance than others; R^2 coefficients were obtained to be equal to 0.82, 0.85, and 0.84 for NDRE, RECI, and MTCI, respectively. Additionally, the performance of the indices in group 3 was better than that in groups 2 and 1. On the contrary, during the second flight, R^2 and RMSE coefficients of the second group of VIs, especially WDRE, were better than those of other groups and indices. It should be noted that WDRE had a weaker performance than other indices during the first and third flights; however, during the second flight, it had the best fitting with plant biomass. This indicated how

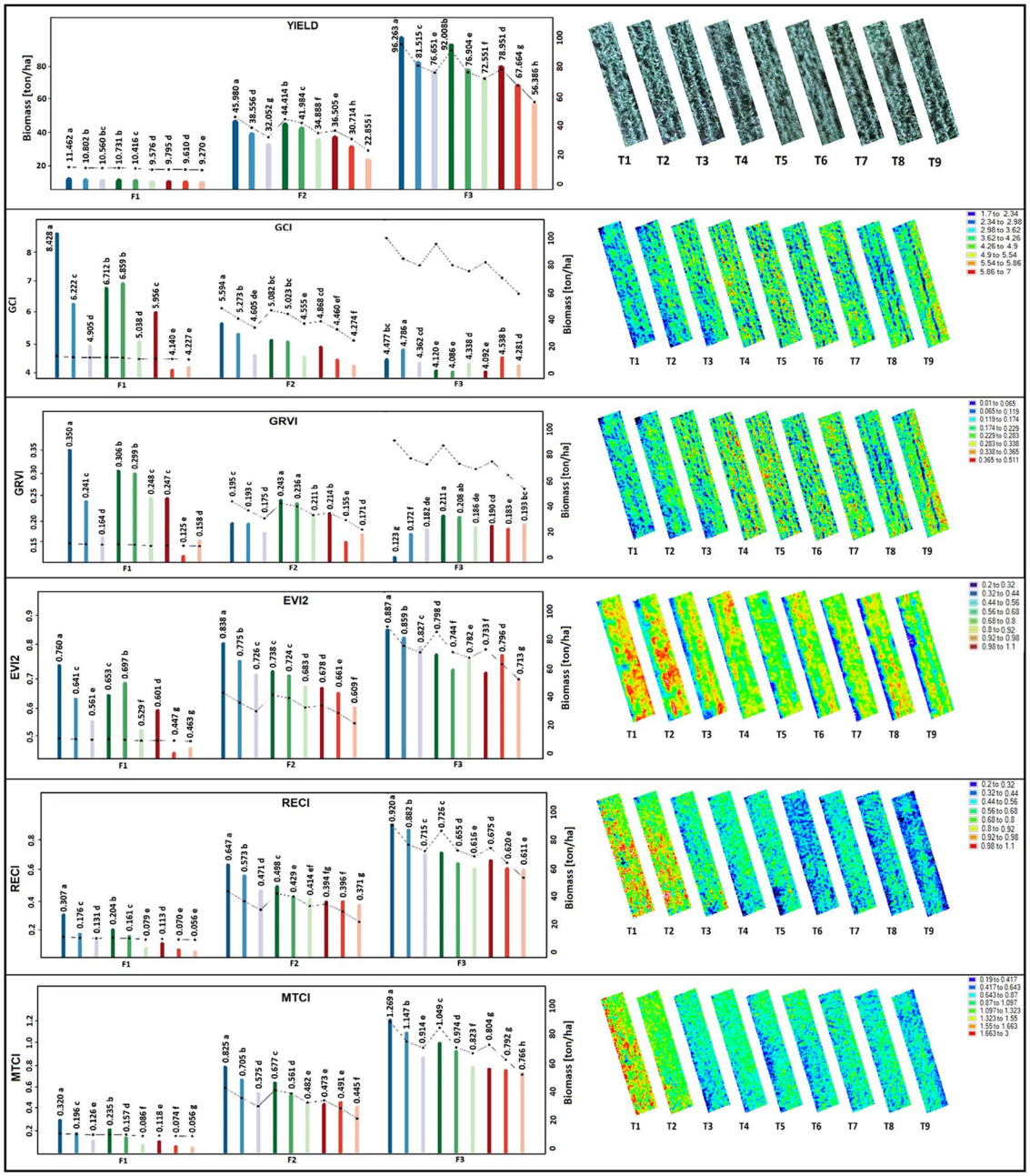

Fig. 5 Comparing means of VIs under irrigation water × N fertilizer interactions

many coefficients used in equations could be effective. Similar to the first flight, in the third flight, the indices of groups 4 and 5 provided a more accurate estimation of corn biomass; however, the R2 and RMSE coefficients were reduced when compared with the first flight results. As mentioned in other researches, the indices were reduced at the end of the growth stages.

However, the results for the entire season showed that the performance of indices was different; four indices including MTCI, RECI, NDRE, and EVI2, with R^2 values of 0.92, 0.89, 0.87, and 0.6,

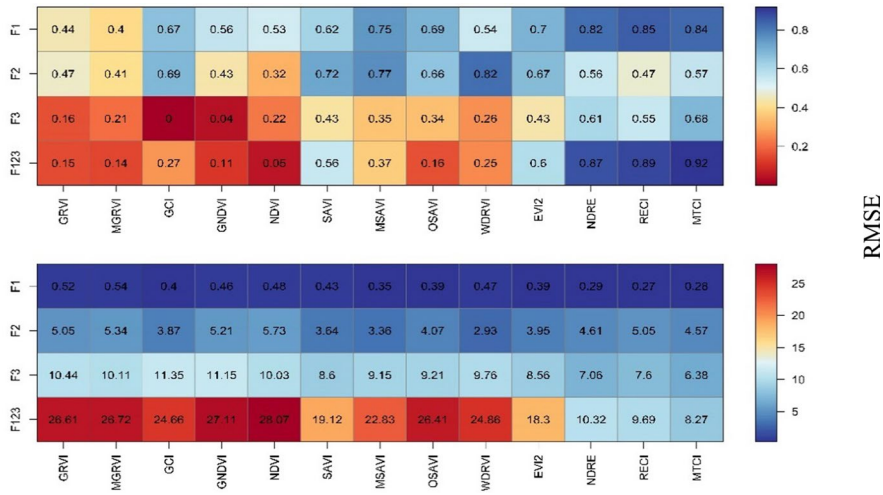

respectively, and the RMSE values of 8.27, 9.69, 10.32, and 18.3 ton/ha, respectively, had the best performance, as compared with other indices. Therefore, the indices of groups 1 and 2, and NDVI, MSAVI, OSAVI, and WDRVI of the third group did not give an accurate estimate of corn biomass during the entire growing season; thus, using these indices for the estimation and comparison of performance could not be suggested in farms with various plantation times.

Figure 7 represents the regression equation of the given fitting for the best indices of each group, along with NDVI, which is widely used in most researches. As can be seen, GRVI, GCI, and NDVI indices were inversely related to corn biomass in the third flight

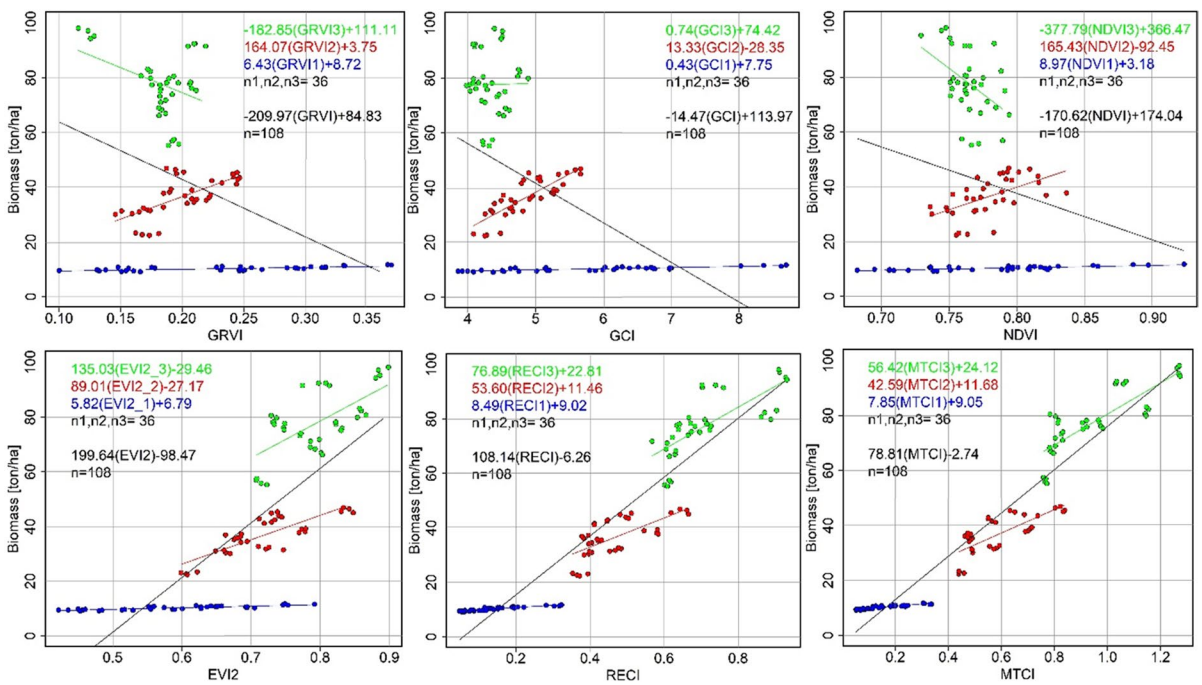

Fig. 7 The relationships for corn biomass and vegetation indices

stage. This could be due to the effect of different irrigation water and N fertilizer levels on the mentioned indices. According to the results represented in Table 3, GRVI for the treatment involving 80% of irrigation water requirement (I2) was more than that for the treatments consisting of the 100% level of irrigation water requirement (I1); further, GCI for the treatments with 60% of irrigation water requirement (I3) was higher than that of the 80% one. Meanwhile, NDVI did not significantly change in the treatments with the irrigation water requirements of 100, 80, and 60%. On the other hand, the effect of N fertilizer levels on spectral indices indicated that GRVI, GCI, and NDVI indices were more in the treatments involving 80 and 60% of the N fertilizer requirement, as compared to those consisting of 100% of the N fertilizer requirement. These factors also caused these indices not to have an acceptable estimate of crop biomass during the growing season; therefore, a negative slope was obtained for the equation of the entire growing season. The R^2 coefficients of GRVI, GCI, and NDVI indices during the entire growing season were obtained to be 0.15, 0.27, and 0.05, respectively; the RMSE values of these indices were also 26.61, 24.66, and 28.07, respectively. On the contrary, examination of EVI2, RECI, and MTCI indices' graphs showed that despite the proper fitting of these indices during the first, second, and third stages, they performed well during the entire growing season. According to the statistical analysis, the effects of different levels of irrigation water and N fertilizer on these spectral indices were observed, and they were raised with an increase in irrigation water and N fertilizer consumption during the growing season. Thus, the R^2 and RMSE coefficients of the entire season were 0.6 and 18.3, respectively for EVI2; these were 0.89 and 9.69, respectively, for RECI. Finally, these were 0.92 and 8.27 for MTCI, respectively.

Therefore, as can be seen, the type and combination of different spectral bands led to different results in crop biomass estimation. For instance, the red-edge reflectance was more sensitive to vegetation chlorophyll in comparison to the red one; with an increase in the consumed nitrogen, the indices based on the red-edge were increased significantly as well. On the other side, the reflectance of the NIR band was highly sensitive to LAI; as the plant was grown, LAI was increased, leading to the rise of reflectance in this spectral range; meanwhile, in the same condition, red-edge reflectance was decreased, reaching the saturation state (Xie et al., 2018).

Estimation of crop biomass using BMA models

To increase the accuracy of the estimation models of corn biomass and to use the advantages of different spectral indices, BMA models were created based on different inputs (Fig. 8). During the selection of the inputs for the BMA models, an attempt was made to choose indices with various bands and best

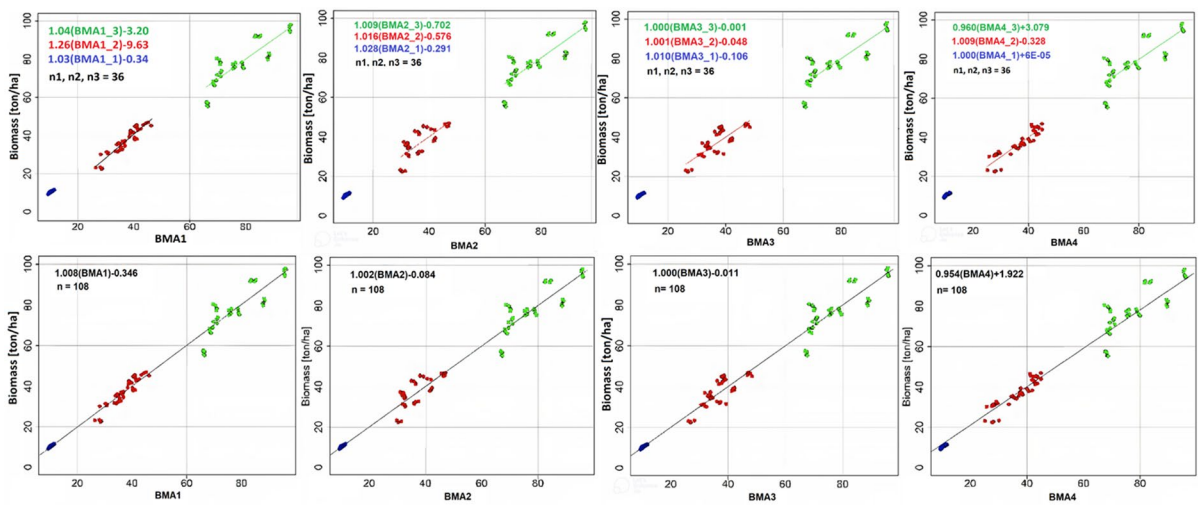

Fig. 8 Relationships for corn biomass and VIs

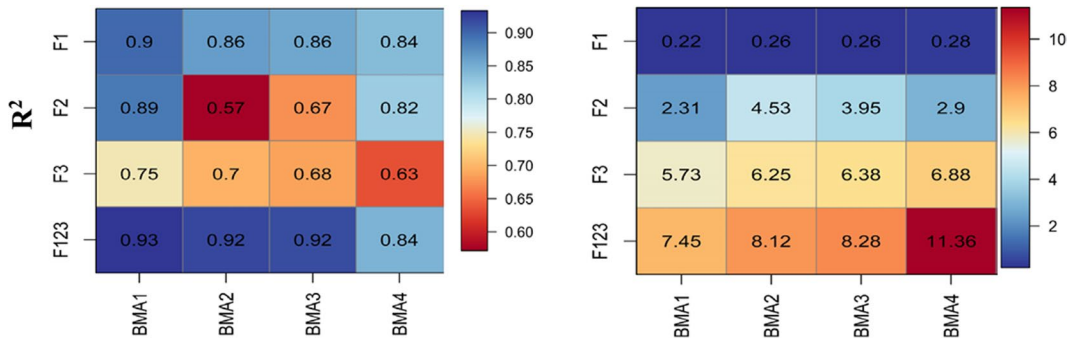

Fig. 9 Coefficients of correlation and RMSE value for BMA models during measurement stages

performance; based on this, four BMA models were selected, as shown below:

- BMA1: MTCI, RECI, MSAVI, GCI, GRVI
- BMA2: MTCI, NDRE, RECI
- BMA3: MTCI, RECI, EVI2
- BMA4: MTCI, WDRVI, GCI

The results showed that BMA1 had the best performance in all three plant growth stages due to the use of 5 vegetation indices. The R^2 coefficients of this model during the first, second ,and third stages were 0.9, 0.89, and 0.75, respectively; also, RMSE values were 0.22, 2.31, and 5.73 ton/ha, respectively (Fig. 9). The BMA2 model had a better performance than BMA3 and BMA4 models in response to not using the NDRE index at the first and third stages. On the contrary, the BMA3 model led to better results, as compared to BMA2 and BMA4 models, due to the use of the EVI2 index, which had a better performance in the second stage in comparison to the indices of groups 4 and 5.

Additionally, examination of the modeling results of crop biomass during the growing season showed that the BMA1 model, with an R^2 value equal to 0.93 and an RMSE value equal to 7.45 ton/ha, had the best results when compared with other indices and BMA models.

Discussion

Studies of different indices showed that using different spectral bands in the form of mathematical relationships with different coefficients could lead to various results whose effects could differ depending on the plant type. It should be noted that most mathematical relationships used for spectral indices are in the fractional form, and the value in the denominator can significantly change the final result (Fig. 4). As can be seen in the indices of group 1, since the green and red bands were used as the denominator of these indices and the average values of these bands at the beginning of the growing season were between 0.055–0.064 and 0.026–0.046, the final value of VIs was higher, while the plant was still at its primary growing stages. This effect was intensified in MGRVI, where its bands were squared. Similarly, regarding the indices of the second group for which red and green bands were used as the denominators, the index value at the beginning of the growing season was obtained to be higher in comparison to that in the following stages since the denominator values were low at the initial stages. In the indices of the third group, the NIR band was used as the denominator and the average range of this spectral band at the beginning of the season was at 0.308–0.523 range; different results were, therefore, obtained. In other words, the value of indices such as SAVI, MSAVI, and EVI2 was in accordance with plant growth at the beginning of the growing season since the utilized coefficients had the raised denominators of their terms. In contrast, this was not the case in other indices of group 3, such as NDVI, OSAVI, and WDRVI (Fig. 4).

On the contrary, NDRE, RECI, and MTCI were raised following plant growth, leading to an increase in the values of the spectral bands. One of the effective factors is the use of the red-edge spectral band in the denominator of indices; the average range of this band was equal to 0.293–0.404, 0.333–0.453, and 0.366–0.495, respectively, throughout the three measurement stages (Fig. 10).

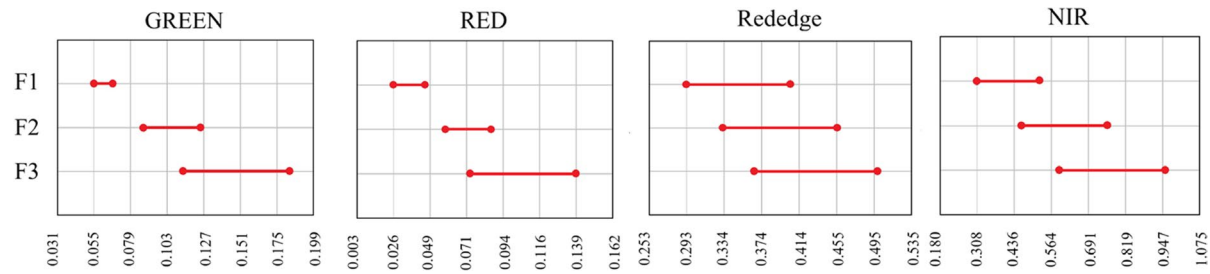

Fig. 10 Changes in reflectance range of spectral bands during different growing stages

Investigation of the effect of irrigation water and nitrogen application levels on VIs showed that in all growing stages, most indices were significantly affected by water and nitrogen levels. However, comparing the means analysis of the treatments showed that changes in some of the indices of groups 1, 2, and 3 were not in accordance with an increase or decrease in irrigation water and nitrogen levels, or the interaction between these two factors. This signified the different effects of irrigation water and nitrogen levels on various spectral indices; some indices such as MTCI, RECI, and NDRE, which included the red-edge spectral bands, could properly indicate the changes in irrigation water and nitrogen. Using indices based on the red-edge spectral band is superior in terms of identifying nitrogen concentration and plant biomass estimation. The spectral range of the red-edge band was from 680 to 750 nm, thus indicating the transition from the chlorophyll absorption band in the red band region to the reflectance range of the NIR region (Clevers et al., 2002). Therefore, in addition to an increase of plant reflectance in this region, sensitivity to plant chlorophyll was higher than that in the red band region (Horler et al., 1983; Xie et al., 2018). Also, comparing the means analysis of the treatments showed that most indices of groups 1, 2, and 3 did not significantly differ during the second and third measurement stages, reaching a saturation state. The results of various studies have shown that the sensitivity of VIs to biophysical parameters such as LAI is reduced as vegetation density is increased to more than a threshold (Gitelson et al., 2002; Small & Lu, 2006). Moreover, similar to our study, Colovic et al. (2022) studied the water and nitrogen status of sweet maize crop by hyperspectral vegetation indices and concluded that red-edge-based indices had higher sensitivity to nitrogen levels, and it is critical to select suitable vegetation indices to monitor the plant eco-physiological response to water and nitrogen stresses.

Examination of the linear regression models also showed the appropriateness of indices in groups 4 and 5 in estimating corn biomass, especially MTCI, thus showing a better performance than other indices by applying three NIR, red-edge, and red spectral bands. Moreover, the effect of relationships and coefficients used in spectral indices was significant. For instance, a comparison of NDVI and EVI2 indices showed that despite using similar spectral bands in these two indices, their performances were significantly different during the entire growing season; NDVI was decreased with plant growth; in contrast, EVI2 was increased directly in proportion to the plant growth. These results were consistent with those obtained by Coelho et al. (2018), who concluded that using NDVI and IRVI indices, with the same red and NIR bands, led to different results in estimating the wheat yield. Vivekar (2019) also carried out a research for estimating crop yield from multispectral UAV images and fixed tower sensors. Based on the obtained results, values of NDVI also were high in the beginning of the crop growth.

Therefore, the type and structure of different spectral bands lead to different results in crop biomass estimation. For instance, the red-edge reflectance is more sensitive to vegetation chlorophyll, and with an increase in the consumed nitrogen, the indices based on the red-edge increase significantly as well. On the other side, NIR is highly sensitive to LAI, and as the plant grows, reflectance of NIR band rises due to LAI increasing (Xie et al., 2018).

According to the different properties of each VI in terms of using various equations, coefficients, and bands, the selection of the best index must be based on a comprehensive analysis, considering the existing limitations and environmental circumstances. On the

other hand, different plants can have various effects on VIs due to their specific and complicated characteristics (Xue & Su, 2017). In addition to the nitrogen concentration and LAI, other parameters such as the structure of leaves and vegetation architecture can be effective on the plants' reflectance. For example, the leaf angle distribution of corn and alfalfa is different from that of wheat and barley (Houborg & Boegh, 2008; Viña et al., 2011). So, by considering these factors, a proper combination of the indices could be used for practical applications. Therefore, using BMA models based on a combination of different indices and utilizing the advantages of each can provide a proper estimation of plant biomass. Based on the results of this research, using the BMA approach can improve the performance of VIs to a significant level.

Conclusion

In recent years, due to the extensive use of remote sensing drones, the qualitative and quantitative monitoring of agricultural farms using this technology and vegetation spectral indices has grown significantly. Given the progress made in designing platforms and sensors, developments of various vegetation indices, as well as the different spectral behaviors of various plants, introducing a comprehensive methodology is essential for farmers and managers to precisely assess crop production. The main objective of this research was to apply different spectral and data-driven approaches to UAV images to identify the efficiency of each technique. For this purpose, in this paper, while examining and analyzing the variation of VIs under different irrigation and nitrogen fertilizer management types, the BMA-based models were used to provide hybrid models for estimating the maize biomass with high accuracy.

Analysis of various VIs showed that using different spectral bands with different coefficients could create various results whose effects might be different during plant growth. Indices such as MTCI, RECI, and NDRE, which include the red-edge spectral bands, could properly indicate variations in irrigation water and nitrogen levels, thus playing a vital role in terms of precision agriculture and saving water and fertilizer resources. For example, during the third flight, the highest values of MTCI resulted in the treatments T1, T2, and T3, which were 1.269, 1.049, and 1.147, respectively; meanwhile, the lowest values were observed in T8 and T9, with values of 0.620 and 0.611, respectively. Also, fitting linear regression models showed the capability of the indices in groups 4 and 5 in estimating corn biomass. Vegetation indices such as MTCI, RECI, NDRE, and EVI2, with R^2 values of 0.92, 0.89, 0.87, and 0.6, respectively, and RMSE values of 8.27, 9.69, 10.32, and 18.3 ton/ha, respectively, had the best performance in estimation corn biomass. Furthermore, some BMA models were developed based on different inputs in order to increase the accuracy of the corn biomass estimation models. The results showed that BMA1 had the best performance in all plant growth stages due to the use of 5 vegetation indices. The R^2 coefficients of this model during the first, second, and third stages were 0.9, 0.89, and 0.75, respectively; also, RMSE values were 0.22, 2.31, and 5.73 ton/ha, respectively. Therefore, the results of BMA models showed that by using such a procedure, we can present high accuracy models for crop yield estimation under different weather conditions, crop types, and agricultural managements.

This research showed that numerous factors such as water and fertilizer management, VIs with different spectral bands and coefficients, and different crop characteristics in terms of vegetation structure and reflectance can cause uncertainty, thus leading to different results in estimating crop biomass. Therefore, instead of selecting specific VIs that are limited to the environmental and managerial conditions of the region, it is necessary to apply the approach of hybrid models that includes all features and benefits of different indices. So, given UAV data availability for precision agriculture, the current research can be considered a progressive research in the domain of agriculture and remote sensing sciences by applying different data-driven approaches and identifying the efficiency of each method.

Author contribution F.F. and S.B. wrote the main manuscript text, B.F. and V.R validated the model, and B.H. edited the analysis tables. All authors reviewed the manuscript.

Funding This research was supported by funds from the Urmia University.

Data availability The datasets generated during and/or analyzed during the current research are available from the corresponding author on reasonable request.

Declarations

Conflict of interest The authors declare no competing interests.

References

Afshar, M. H., Al-Yaari, A., & Yilmaz, M. T. (2021a). Comparative evaluation of microwave L-band VOD and optical NDVI for agriculture drought detection over Central Europe. *Remote Sensing, 13*(7), 1251.

Afshar, M. H., Foster, T., Higginbottom, T. P., Parkes, B., Hufkens, K., Mansabdar, S., Ceballos, F., & Kramer, B. (2021b). Improving the performance of index insurance using crop models and phenological monitoring. *Remote Sensing, 13*(5), 924.

Baio, F. H. R., Neves, D. C., da Silva Campos, C. N., & Teodoro, P. E. (2018). Relationship between cotton productivity and variability of NDVI obtained by Landsat images. *Bioscience Journal*, *34*(6).

Becker-Reshef, I., Vermote, E., Lindeman, M., & Justice, C. (2010). A generalized regression-based model for forecasting winter wheat yields in Kansas and Ukraine using MODIS data. *Remote Sensing of Environment, 114*(6), 1312–1323.

Bendig, J., Yu, K., Aasen, H., Bolten, A., Bennertz, S., Broscheit, J., Gnyp, M. L., & Bareth, G. (2015). Combining UAV-based plant height from crop surface models, visible, and near infrared vegetation indices for biomass monitoring in barley. *International Journal of Applied Earth Observation and Geoinformation, 39*, 79–87.

Bolton, D. K., & Friedl, M. A. (2013). Forecasting crop yield using remotely sensed vegetation indices and crop phenology metrics. *Agricultural and Forest Meteorology, 173*, 74–84.

Carneiro, F. M., Furlani, C. E. A., Zerbato, C., de Menezes, P. C., da Silva Gírio, L. A., & de Oliveira, M. F. (2019). Comparison between vegetation indices for detecting spatial and temporal variabilities in soybean crop using canopy sensors. *Precision Agriculture*, 1-29.

Chen, A., Orlov-Levin, V., & Meron, M. (2019). Applying high-resolution visible-channel aerial imaging of crop canopy to precision irrigation management. *Agricultural Water Management, 216*, 196–205.

Clevers, J., De Jong, S., Epema, G., Van Der Meer, F., Bakker, W., Skidmore, A., & Scholte, K. (2002). Derivation of the red edge index using the MERIS standard band setting. *International Journal of Remote Sensing, 23*(16), 3169–3184.

Coelho, A. P., Rosalen, D. L., Faria, R. T. D. (2018). Vegetation indices in the prediction of biomass and grain yield of white oat under irrigation levels. *Pesquisa Agropecuária Tropical, 48*(2), 109–117.

Colovic, M., Yu, K., Todorovic, M., Cantore, V., Hamze, M., Albrizio, R., & Stellacci, A. M. (2022). Hyperspectral vegetation indices to assess water and nitrogen status of sweet maize crop. *Agronomy, 12*(9), 2181.

Córcoles, J. I., Ortega, J. F., Hernández, D., & Moreno, M. A. (2013). Estimation of leaf area index in onion (Allium cepa L.) using an unmanned aerial vehicle. *Biosystems engineering*, *115*(1), 31-42.

Dash, J., & Curran, P. (2004). The MERIS terrestrial chlorophyll index.

Duan, B., Fang, S., Gong, Y., Peng, Y., Wu, X., & Zhu, R. (2021). Remote estimation of grain yield based on UAV data in different rice cultivars under contrasting climatic zone. *Field Crops Research, 267*, 108148.

Duncan, J. M., Dash, J., & Atkinson, P. M. (2015). Elucidating the impact of temperature variability and extremes on cereal croplands through remote sensing. *Global change biology, 21*(4), 1541–1551.

Feizizadeh, B., Garajeh, M. K., Lakes, T., & Blaschke, T. (2021). A deep learning convolutional neural network algorithm for detecting saline flow sources and mapping the environmental impacts of the Urmia Lake drought in Iran. *Catena, 207*, 105585.

Fullana-Pericàs, M., Conesa, M. À., Gago, J., Ribas-Carbó, M., & Galmés, J. (2022). High-throughput phenotyping of a large tomato collection under water deficit: Combining UAVs' remote sensing with conventional leaf-level physiologic and agronomic measurements. *Agricultural Water Management, 260*, 107283.

Geipel, J., Link, J., & Claupein, W. (2014). Combined spectral and spatial modeling of corn yield based on aerial images and crop surface models acquired with an unmanned aircraft system. *Remote Sensing, 6*(11), 10335–10355.

Gitelson, A., & Merzlyak, M. N. (1994). Quantitative estimation of chlorophyll-a using reflectance spectra: Experiments with autumn chestnut and maple leaves. *Journal of Photochemistry and Photobiology B: Biology, 22*(3), 247–252.

Gitelson, A., Stark, R., Grits, U., Rundquist, D., Kaufman, Y., & Derry, D. (2002). Vegetation and soil lines in visible spectral space: A concept and technique for remote estimation of vegetation fraction. *International Journal of Remote Sensing, 23*(13), 2537–2562.

Gitelson, A. A., Gritz, Y., & Merzlyak, M. N. (2003). Relationships between leaf chlorophyll content and spectral reflectance and algorithms for non-destructive chlorophyll assessment in higher plant leaves. *Journal of plant physiology, 160*(3), 271–282.

Hoeting, J. A., Madigan, D., Raftery, A. E., & Volinsky, C. T. (1999). Bayesian model averaging: A tutorial. *Statistical Science*, 382-401.

Horler, D., & Dockray, M., & Barber, J. (1983). The red edge of plant leaf reflectance. *International Journal of Remote Sensing, 4*(2), 273–288.

Houborg, R., & Boegh, E. (2008). Mapping leaf chlorophyll and leaf area index using inverse and forward canopy reflectance modeling and SPOT reflectance data. *Remote Sensing of Environment, 112*(1), 186–202.

Huang, J., Wang, X., Li, X., Tian, H., & Pan, Z. (2013). Remotely sensed rice yield prediction using multi-temporal NDVI data derived from NOAA's-AVHRR. *PloS one, 8*(8), e70816.

Huete, A. R. (1988). A soil-adjusted vegetation index (SAVI). *Remote Sensing of Environment, 25*(3), 295–309.

Ihuoma, S. O., & Madramootoo, C. A. (2017). Recent advances in crop water stress detection. *Computers and Electronics in Agriculture, 141*, 267–275.

Jiang, Z., Huete, A. R., Didan, K., & Miura, T. (2008). Development of a two-band enhanced vegetation index without a blue band. *Remote Sensing of Environment, 112*(10), 3833–3845.

Jorge, J., Vallbé, M., & Soler, J. A. (2019). Detection of irrigation inhomogeneities in an olive grove using the NDRE vegetation index obtained from UAV images. *European Journal of Remote Sensing, 52*(1), 169–177.

Li, B., Xu, X., Zhang, L., Han, J., Bian, C., Li, G., Liu, J., & Jin, L. (2020). Above-ground biomass estimation and yield prediction in potato by using UAV-based RGB and hyperspectral imaging. *ISPRS Journal of Photogrammetry and Remote Sensing, 162*, 161–172.

Lisar, S. Y., Motafakkerazad, R., Hossain, M. M., & Rahman, I. M. (2012). Causes, effects and responses. *Water stress*, 1.

Lobell, D. B. (2013). The use of satellite data for crop yield gap analysis. *Field Crops Research, 143*, 56–64.

Maresma, A., Chamberlain, L., Tagarakis, A., Kharel, T., Godwin, G., Czymmek, K. J., Shields, E., & Ketterings, Q. M. (2020). Accuracy of NDVI-derived corn yield predictions is impacted by time of sensing. *Computers and Electronics in Agriculture, 169*, 105236.

Mkhabela, M., Bullock, P., Raj, S., Wang, S., & Yang, Y. (2011). Crop yield forecasting on the Canadian Prairies using MODIS NDVI data. *Agricultural and Forest Meteorology, 151*(3), 385–393.

Noureldin, N., Aboelghar, M., Saudy, H., & Ali, A. (2013). Rice yield forecasting models using satellite imagery in Egypt. *The Egyptian Journal of Remote Sensing and Space Science, 16*(1), 125–131.

Peñuelas, J., Gamon, J., Fredeen, A., Merino, J., & Field, C. (1994). Reflectance indices associated with physiological changes in nitrogen-and water-limited sunflower leaves. *Remote Sensing of Environment, 48*(2), 135–146.

Qi, J., Chehbouni, A., Huete, A. R., Kerr, Y. H., & Sorooshian, S. (1994). A modified soil adjusted vegetation index. *Remote Sensing of Environment, 48*(2), 119–126.

Raftery, A. E., Gneiting, T., Balabdaoui, F., & Polakowski, M. (2005). Using Bayesian model averaging to calibrate forecast ensembles. *Monthly weather review, 133*(5), 1155–1174.

Rouse, J. W., Haas, R. H., Schell, J. A., Deering, D. W., & Harlan, J. C. (1974). Monitoring the vernal advancement and retrogradation (green wave effect) of natural vegetation. *NASA/GSFC Type III Final Report, Greenbelt, Md*, *371*.

Sharifi, A. (2020). Remotely sensed vegetation indices for crop nutrition mapping. *Journal of the Science of Food and Agriculture, 100*(14), 5191–5196.

Small, C., & Lu, J. W. (2006). Estimation and vicarious validation of urban vegetation abundance by spectral mixture analysis. *Remote Sensing of Environment, 100*(4), 441–456.

Teoh, C., Nadzim, N. M., Shahmihaizan, M. M., Izani, I. M. K., Faizal, K., & Shukry, H. M. (2016). Rice yield estimation using below cloud remote sensing images acquired by unmanned airborne vehicle system. *International Journal on Advanced Science, Engineering and Information Technology, 6*(4), 516–519.

Tian, H., Wang, P., Tansey, K., Zhang, S., Zhang, J., & Li, H. (2020). An IPSO-BP neural network for estimating wheat yield using two remotely sensed variables in the Guanzhong Plain, PR China. *Computers and Electronics in Agriculture, 169*, 105180.

Tucker, C. J. (1979). Red and photographic infrared linear combinations for monitoring vegetation. *Remote Sensing of Environment, 8*(2), 127–150.

Turner, D., Lucieer, A., & Watson, C. (2012). An automated technique for generating georectified mosaics from ultra-high resolution unmanned aerial vehicle (UAV) imagery, based on structure from motion (SfM) point clouds. *Remote Sensing, 4*(5), 1392–1410.

Verger, A., Vigneau, N., Chéron, C., Gilliot, J.-M., Comar, A., & Baret, F. (2014). Green area index from an unmanned aerial system over wheat and rapeseed crops. *Remote Sensing of Environment, 152*, 654–664.

Viero, F., Menegati, G. B., Carniel, E., Silva, P. R. F. D., & Bayer, C. (2017). Urease inhibitor and irrigation management to mitigate ammonia volatilization from urea in no-till corn. *Revista Brasileira de Ciência do Solo*, *41*.

Viña, A., Gitelson, A. A., Nguy-Robertson, A. L., & Peng, Y. (2011). Comparison of different vegetation indices for the remote assessment of green leaf area index of crops. *Remote Sensing of Environment, 115*(12), 3468–3478.

Vivekar, A. (2019). *Evaluation of methodology for estimating crop yield from multispectral UAV images* Lund University].

Wang, Y.-P., Chang, K.-W., Chen, R.-K., Lo, J.-C., & Shen, Y. (2010). Large-area rice yield forecasting using satellite imageries. *International Journal of Applied Earth Observation and Geoinformation, 12*(1), 27–35.

Willmott, C. J., & Matsuura, K. (2005). Advantages of the mean absolute error (MAE) over the root mean square error (RMSE) in assessing average model performance. *Climate research, 30*(1), 79–82.

Xie, Q., Dash, J., Huang, W., Peng, D., Qin, Q., Mortimer, H., Casa, R., Pignatti, S., Laneve, G., & Pascucci, S. (2018). Vegetation indices combining the red and red-edge spectral information for leaf area index retrieval. *IEEE Journal of selected topics in applied earth observations and remote sensing, 11*(5), 1482–1493.

Xu, X., Nie, C., Jin, X., Li, Z., Zhu, H., Xu, H., Wang, J., Zhao, Y., & Feng, H. (2021). A comprehensive yield evaluation indicator based on an improved fuzzy comprehensive evaluation method and hyperspectral data. *Field Crops Research, 270*, 108204.

Xue, J., & Su, B. (2017). Significant remote sensing vegetation indices: A review of developments and applications. *Journal of Sensors*, *2017*.

Yeom, J., Jung, J., Chang, A., Ashapure, A., Maeda, M., Maeda, A., & Landivar, J. (2019). Comparison of vegetation indices derived from UAV data for differentiation of tillage effects in agriculture. *Remote Sensing, 11*(13), 1548.

Zhang, C., & Kovacs, J. M. (2012). The application of small unmanned aerial systems for precision agriculture: A review. *Precision Agriculture, 13*(6), 693–712.

Zhao, B., Duan, A., Ata-Ul-Karim, S. T., Liu, Z., Chen, Z., Gong, Z., Zhang, J., Xiao, J., Liu, Z., & Qin, A. (2018). Exploring new spectral bands and vegetation indices for estimating nitrogen nutrition index of summer maize. *European Journal of Agronomy, 93*, 113–125.

Zhao, Y., Potgieter, A. B., Zhang, M., Wu, B., & Hammer, G. L. (2020). Predicting wheat yield at the field scale by combining high-resolution Sentinel-2 satellite imagery and crop modelling. *Remote Sensing, 12*(6), 1024.

Zhou, X., Wang, P., Tansey, K., Zhang, S., Li, H., & Tian, H. (2020). Reconstruction of time series leaf area index for improving wheat yield estimates at field scales by fusion of Sentinel-2,-3 and MODIS imagery. *Computers and Electronics in Agriculture, 177*, 105692.

Zhou, X., Zheng, H., Xu, X., He, J., Ge, X., Yao, X., Cheng, T., Zhu, Y., Cao, W., & Tian, Y. (2017). Predicting grain yield in rice using multi-temporal vegetation indices from UAV-based multispectral and digital imagery. *ISPRS Journal of Photogrammetry and Remote Sensing, 130*, 246–255.

Zhou, Y., Lao, C., Yang, Y., Zhang, Z., Chen, H., Chen, Y., Chen, J., Ning, J., & Yang, N. (2021). Diagnosis of winter-wheat water stress based on UAV-borne multi-spectral image texture and vegetation indices. *Agricultural Water Management, 256*, 107076.

Zou, K. H., Tuncali, K., & Silverman, S. G. (2003). Correlation and simple linear regression. *Radiology, 227*(3), 617–628.